41. Morizane C, Adachi K, Furutani I, Fujita Y, Akaike A, Kashii S, Honda Y (1997) N(omega)-nitro-L-arginine methyl ester protects retinal neurons against N-methyl-D-aspartate-induced neurotoxicity in vivo. Eur J Pharmacol 328:45–49
42. Musashi K, Kiryu J, Miyamoto K, Miyahara S, Katsuta H, Tamura H, Hirose F, Yoshimura N (2005) Thrombin inhibitor reduces leukocyte-endothelial cell interactions and vascular leakage after scatter laser photocoagulation. Invest Ophthalmol Vis Sci 46:2561–2566
43. Nishijima K, Kiryu J, Tsujikawa A, Miyamoto K, Honjo M, Tanihara H, Nonaka A, Yamashiro K, Katsuta H, Miyahara S, Honda Y, Ogura Y (2004) Platelets adhering to the vascular wall mediate postischemic leukocyte-endothelial cell interactions in retinal microcirculation. Invest Ophthalmol Vis Sci 45:977–984
44. Olson MF (2004) Contraction reaction: mechanical regulation of Rho GTPase. Trends Cell Biol 14:111–114
45. Osborne NN, Larsen AK (1996) Antigens associated with specific retinal cells are affected by ischaemia caused by raised intraocular pressure: effect of glutamate antagonists. Neurochem Int 29:263–270
46. Osborne NN, Wood JP, Melena J, Chao HM, Nash MS, Bron AJ, Chidlow G (2000) 5-Hydroxytryptamine1A agonists: potential use in glaucoma. Evidence from animal studies. Eye 14:454–463
47. Osborne NN, Chidlow G, Layton CJ, Wood JP, Casson RJ, Melena J (2004) Optic nerve and neuroprotection strategies. Eye 18:1075–1084
48. Penfold PL, Madigan MC, Gillies MC, Provis JM (2001) Immunological and aetiological aspects of macular degeneration. Prog Retin Eye Res 20:385–414
49. Rosenbaum DM, Rosenbaum PS, Gupta A, Michaelson MD, Hall DH, Kessler JA (1997) Retinal ischemia leads to apoptosis which is ameliorated by aurintricarboxylic acid. Vision Res 37:3445–3451
50. Sawada A, Neufeld AH (1999) Confirmation of the rat model of chronic, moderately elevated intraocular pressure. Exp Eye Res 69:525–531
51. Springer TA (1994) Traffic signals for lymphocyte recirculation and leukocyte emigration: the multistep paradigm. Cell 76:301–314
52. Sucher NJ, Lipton SA, Dreyer EB (1997) Molecular basis of glutamate toxicity in retinal ganglion cells. Vision Res 37:3483–3493
53. Szabo ME, Droy-Lefaix MT, Doly M, Carre C, Braquet P (1991) Ischemia and reperfusion-induced histologic changes in the rat retina. Demonstration of a free radical-mediated mechanism. Invest Ophthalmol Vis Sci 32:1471–1478
54. Szabo ME, Droy-Lefaix MT, Doly M, Braquet P (1992) Ischaemia- and reperfusion-induced Na+, K+, Ca2+ and Mg2+ shifts in rat retina: effects of two free radical scavengers, SOD and EGB 761. Exp Eye Res 55:39–45
55. Tamura H, Miyamoto K, Kiryu J, Miyahara S, Katsuta H, Hirose F, Musashi K, Yoshimura N (2005) Intravitreal injection of corticosteroid attenuates leukostasis and vascular leakage in experimental diabetic retina. Invest Ophthalmol Vis Sci 46:1440–1444
56. Tsujikawa A, Ogura Y, Hiroshiba N, Miyamoto K, Kiryu J, Tojo SJ, Miyasaka M, Honda Y (1999) Retinal ischemia-reperfusion injury attenuated by blocking of adhesion molecules of vascular endothelium. Invest Ophthalmol Vis Sci 40:1183–1190
57. Wittchen ES, van Buul JD, Burridge K, Worthylake RA (2005) Trading spaces: Rap, Rac, and Rho as architects of transendothelial migration. Curr Opin Hematol 12:14–21
58. Wojciak-Stothard B, Potempa S, Eichholtz T, Ridley AJ (2001) Rho and Rac but not Cdc42 regulate endothelial cell permeability. J Cell Sci 114:1343–1355
59. Worthylake RA, Burridge K (2001) Leukocyte transendothelial migration: orchestrating the underlying molecular machinery. Curr Opin Cell Biol 13:569–577
60. Yeh DC, Bula DV, Miller JW, Gragoudas ES, Arroyo JG (2004) Expression of leukocyte adhesion molecules in human subfoveal choroidal neovascular membranes treated with and without photodynamic therapy. Invest Ophthalmol Vis Sci 45:2368–2373
61. Zhang Y, Cho CH, Atchaneeyasakul LO, McFarland T, Appukuttan B, Stout JT (2005) Activation of the mitochondrial apoptotic pathway in a rat model of central retinal artery occlusion. Invest Ophthalmol Vis Sci 46:2133–2139

Potential Role of Rho-Associated Protein Kinase Inhibitor Y-27632 in Glaucoma Filtration Surgery

Megumi Honjo,[1] *Hidenobu Tanihara,*[2] *Takanori Kameda,*[1] *Takahiro Kawaji,*[2] *Nagahisa Yoshimura,*[1] *and Makoto Araie*[3]

Purpose. To investigate the role of Y-27632, a specific inhibitor of Rho-associated protein kinase (ROCK) in regulating human Tenon fibroblast (HTF) activities including proliferation, adhesion, contraction, migratory response, and myofibroblast transdifferentiation. Effects of Y-27632 on prevention of postoperative scar formation were also examined in a rabbit model of glaucoma filtration surgery.

Methods. After treatment of HTFs with Y-27632, cell toxicity, proliferation, migration, adhesion, and contraction were studied. The cytoskeleton and α-smooth muscle actin (α-SMA) expression were examined via immunohistochemistry. In vivo studies in Japanese white rabbits consisted of a full-thickness sclerostomy followed in the 7-day postoperative period by topical application of Y-27632. Intraocular pressure, morphologic changes in bleb features, and histology of surgical sites were evaluated.

Results. Y-27632 had no direct toxicity or significant effects on cell proliferation of HTF. The cell adhesion assay showed that Y-27632 promoted adhesiveness to both fibronectin and collagen type I. Use of Y-27632 significantly inhibited collagen gel contraction and α-SMA expression in HTFs. Y-27632 also increased HTF motility. In vivo, Y-27632 inhibited wound healing and fibroproliferation after filtration surgery and significantly improved surgical outcome compared with the vehicle. Histologic examination revealed that blebs in the Y-27632-treated group differed from those in the vehicle-treated group in that they lacked significant collagen deposition in the sclerostomy area.

Conclusions. Y-27632 had profound effects on activities of HTFs and was effective in preventing fibroproliferation and scar formation in a rabbit model of glaucoma surgery. A ROCK inhibitor may be an effective anti-scarring agent after glaucoma filtering surgery. (*Invest Ophthalmol Vis Sci.* 2007;48: 5549-5557) DOI:10.1167/iovs.07-0878

From the [1]Department of Ophthalmology and Visual Sciences, Kyoto University Graduate School of Medicine, Kyoto, Japan; the [2]Department of Ophthalmology and Visual Science, Kumamoto University Graduate School of Medical Sciences, Kumamoto, Japan; the [3]Department of Ophthalmology, Graduate School of Medicine, University of Tokyo, Tokyo, Japan.

Supported by a Grant in Aid for Scientific Research from the Japan Society for the Promotion of Science (JSPS).

Submitted for publication July 13, 2007; revised August 16, 2007; accepted October 4, 2007.

Disclosure: **M. Honjo**, None; **H. Tanihara**, None; **T. Kameda**, None; **T. Kawaji**, None; **N. Yoshimura**, None; **M. Araie**, None

The publication costs of this article were defrayed in part by page charge payment. This article must therefore be marked "*advertisement*" in accordance with 18 U.S.C. §1734 solely to indicate this fact.

Corresponding author: Megumi Honjo, Department of Ophthalmology and Visual Sciences, Kyoto University Graduate School of Medicine, 54 Kawahara-cho, Shogoin, Sakyo, 606-8507, Kyoto, Japan; m_honjo@kuhp.kyoto-u.ac.jp.

The main cause of failure of glaucoma filtration surgery is postoperative scarring in the filtering bleb. Perioperative administration of antimetabolites such as 5-fluorouracil and mitomycin C (MMC) is effective in limiting the scarring process. However, use of these antiproliferative agents is accompanied by severe side effects.[1] Fibroblasts from the subconjunctival space play a key role in the scarring process. Several agents, such as antibody against transforming growth factor (TGF)-β2,[2] alkylphosphocholines,[3] and p38 inhibitors,[4] are reportedly potential alternative antiscarring therapeutic substances, in that they can regulate activities of fibroblasts, but they are not yet available for routine clinical use.

Fibroblasts generate a contractile force, which is essential for their role in the postoperative scarring process.[5] In addition, transdifferentiation of fibroblasts into myofibroblasts is a crucial step in wound healing and scar formation,[6] which is associated with expression of α-smooth muscle actin (α-SMA).[7] Enhanced α-SMA expression indicates the presence of activated fibroblasts with increased synthesis of extracellular matrix (ECM) proteins, growth factors, and integrins.[4,8]

The Rho subfamily of small GTPases (including Rho and Rac) has critical functions in regulation of actomyosin cytoskeletal organization, cell adhesion, and cell motility.[9-12] The cytoskeleton is regarded as a primary target of growth factor action and mediates several cell responses to the ECM.[10,13,14] ROCK I, one of the putative target molecules of Rho, has been identified as a Rho effector.[15] ROCKs are important for regulating focal adhesions and stress fiber formation in cultured fibroblasts and epithelial cells.[16,17] We have reported that a specific inhibitor of ROCK I, Y-27632, causes significantly reduced intraocular pressure (IOP) in rabbits and altered cell shape and the actin cytoskeleton of cultured human trabecular meshwork (TM) cells.[18] We have also demonstrated that Y-27632 has profound effects on TM cell activities.[19] In addition, Rho has been implicated in pathologic wound healing.[20]

We hypothesize that Rho plays an important role in modulation of cytoskeletal dynamics in human Tenon fibroblasts (HTFs) and thereby influences HTF activities. Although some research has implicated TGF-β-mediated growth factors in modification of HTF activities,[4,21] the effects of ROCK inhibitors on cytoskeletal organization, proliferation, and transdifferentiation into myofibroblasts in HTFs have not been fully explored. In particular, the involvement of the Rho signaling pathways in mediating such effects in animal models is unknown. Therefore, in this study we used Y-27632 to test its ability to inhibit proliferation, migration, and contraction of HTFs without toxicity. We also investigated its effect on preventing fibroproliferation and scar formation in a rabbit model of glaucoma surgery. These results suggest that this ROCK inhibitor may effectively prevent postoperative filtration bleb failure in glaucoma surgery.

Materials and Methods

Culture of HTFs

Small Tenon biopsy specimens were obtained during standard cataract surgery after selected patients had received comprehensive informa-

Copyright © Association for Research in Vision and Ophthalmology

tion and provided written consent for the procedure. The protocol was approved by the Institutional Review Board at Kyoto University in compliance with tenets of the Declaration of Helsinki. Primary HTFs obtained from expansion cultures of the Tenon explants were propagated in Dulbecco's modified Eagle's medium (DMEM) supplemented with 10% heat-inactivated fetal calf serum and antibiotics. Cells were maintained in the logarithmic growth phase, and cells from passages 3 to 6 were used in all experiments, which were performed at least three times with similar results.

Trypan Blue Exclusion Test

The cytotoxicity of Y-27632 was evaluated via a trypan blue exclusion test. Viable cells were counted in vitro according to a previously described method.[19,22] Briefly, 5×10^5 HTFs were plated and grown for 24 hours, then treated with or without Y-27632 (1, 10, or 100 μM) for 24 hours. After trypan blue treatment, stained, and unstained cells were counted by using a hematocytometer. The percentage of cell viability was calculated according to the following formula: % cell viability = (viable cell count/total cell count) × 100. Five independent experiments were performed.

Cell Proliferation Assay

Proliferation of cultured HTFs was measured by use of the commercially available MTT (3-(4,5-dimethyl-2-thiazyl)-2, 5-diphenyl-2*H*-tetrazolium bromide) cell proliferation kit (Nacalai Tesque, Kyoto, Japan), according to the manufacturer's instructions. Cells were plated at a density of 1×10^4 cells per well in 96-well plates and were allowed to adhere for 24 hours. After cultures were washed with phosphate-buffered saline (PBS), they were incubated with or without Y-27632 (1, 10, or 100 μM) for 72 hours and then treated with 5 mg/mL MTT for 4 hours at 37°C. The relative active number of cells was determined by an automated plate reader (Bio-Rad, Hercules, CA).

Cell Adhesion Assay

The cell adhesion assay was performed as previously described.[19,23] Wells in 96-well plates were coated overnight with 10 μg/mL fibronectin (Sigma-Aldrich-Aldrich, St. Louis, MO) or 0.5 μg/mL collagen type I (Calbiochem, San Diego, CA) at 4°C. Remaining binding sites were blocked by 0.1% bovine serum albumin (BSA) in PBS. HTFs in culture medium containing 2 mg/mL BSA with or without Y-27632 (1, 10, or 100 μM) were loaded onto coated wells at 4×10^4 cells per well. After incubation for 60 minutes, unattached cells were removed and washed with PBS. Then, 100 μL of calcein-AM solution (Calbiochem) was added to each well and incubated for 60 minutes. The relative remaining number of cells was determined by an automated plate reader (Bio-Rad).

Collagen Gel Contraction Assay

This assay was performed as previously described,[19,24,25] with minor modifications. Briefly, HTFs were trypsinized and resuspended in culture medium at a density of 2.2×10^6 cells/mL, with or without Y-27632 (1, 10, or 100 μM). Collagen type I (Nitta Gelatin, Osaka, Japan), 10 × DMEM, reconstitution buffer (Nitta Gelatin), HTF cell suspension, and water were mixed in an ice bath at a ratio of 7:1:1:1. Aliquots (0.5 mL) of the resultant mixture were added to each well of 1% BSA-coated 24-well clusters and collagen gel formation was induced. DMEM (0.5 mL), with or without Y-27632 (1, 10, or 100 μM), was then placed on top of the collagen gels. After 1 hour of incubation, gels were freed from the walls of the culture wells, and diameters of the gels were scanned into a computer and measured every 24 hours for 4 days.

Immunohistochemistry

HTFs were plated on glass coverslips, cultured overnight, and then serum starved for 24 hours. Then, 10 μM lysophospholipid acid (LPA; Sigma-Aldrich) was added for 10 minutes, after which it was incubated with Y-27632 (1, 10, or 100 μM) for 30 minutes. After this exposure, the cells were fixed in 2% paraformaldehyde-PBS for 15 minutes and then blocked in 2% BSA for 30 minutes. Coverslips were incubated with anti-vinculin antibody (Sigma-Aldrich) or α-SMA antibody (Dako Japan, Kyoto, Japan) for 30 minutes. Rhodamine-phalloidin (Invitrogen-Molecular Probes, Eugene, OR) was used to counterstain the F-actin cytoskeleton. Samples were washed with PBS and incubated with FITC-conjugated secondary antibody (Chemicon, Temecula, CA) for 30 minutes. After they were washed, the cells were mounted in antifade medium and observed via the fluorescence microscope (model IX71; Olympus, Tokyo, Japan). Immunohistochemistry with rabbit specimens used the same routine procedure.

Measurement of Cell Motility Activities

HTFs were grown to confluence in 100-mm tissue culture dishes. Three or four sites in each dish were scraped with a yellow plastic pipette tip to remove the confluent cells and create a linear line. Medium was replaced with fresh medium, with or without Y-27632 (1, 10, or 100 μM). After incubation at 37°C for 9 hours, the movement of cells into the wound area was photographed by a digital microscope camera (Olympus) and analyzed via computer software (Olympus). The shortest distance between the edges of migrated HTFs (including protrusions) from both sides was measured, as previously described.[19,26]

Animals and Sclerostomy Protocol

Twelve female Japanese White rabbits (*Pasteurella* free, each 2.0 to 2.4 kg, 12 to 14 weeks old; SRC Japan, Osaka, Japan) were used. Experiments were conducted according to guidelines of the ARVO Statement for the Use of Animals in Ophthalmic and Vision Research and approved by the Animal Use Committee at Kyoto University. All investigations involving rabbits, including surgery, IOP measurements, bleb scoring, and determination of histologic features, were conducted in a blinded manner.

Rabbits were anesthetized with an intramuscular injection of ketamine hydrochloride (5 mg/kg body weight), and xylazine hydrochloride (5 mg/kg body weight). A limbus-based flap of the conjunctiva and the Tenon capsule was made at a distance of 5 mm from the limbus in the superior nasal quadrant of the right eye. A sclerostomy was performed, and a fistula was constructed toward the anterior chamber. The conjunctiva was closed with three 8-0 polyglactin 910 sutures. After bleb formation was tested, topical Y-27632 or PBS (12 μL of eye drops of 10 mM Y-27632 or the same amount of PBS) was applied to the eye. After surgery, 1 cm of 3 mg/g ofloxacin ointment was applied to the eye. Topical Y-27632 or PBS was applied for 7 postoperative days.

Clinical Evaluation of Postoperative Y-27632 Effects in a Rabbit Model of Glaucoma Filtration Surgery

Glaucoma Filtration Surgery. Baseline observations were obtained before surgery. The IOP of the rabbit eye was measured during topical instillation of anesthetic before and after surgery by using an applanation tonometer (Tonovet; Tiolat, Helsinki, Finland). IOP was monitored daily for 7 postoperative days, with values obtained at the same time each day. Blebs were examined via a slit lamp and were graded as previously described by Perkins et al.,[27] according to a qualitative scale of 1+ to 4+, reflecting increasing bleb height and size as follows: 1+, minimal height, conjunctiva thickening, no microcysts; 2+, microcysts present; 3+, elevated bleb covering 2 to 3 clock hours of the eye; and 4+, greatly elevated bleb covering more than 4 clock hours. A score of 0 indicated no observable bleb. Bleb failure was defined as the appearance of a flat, vascularized, scarred bleb in the presence of a deep anterior chamber.

Histologic Evaluation. For this study, rabbits were killed humanely 7 days after surgery. An incision was made 90° away from the

surgical site, and the whole globe was fixed in 4% paraformaldehyde in PBS for 48 hours at 4°C and was then embedded in medium (Tissue-Tek; Sakura Finetechnical, Tokyo, Japan). Serial sections were cut through the sclerostomy site. Approximately every fifth section was stained with standard hematoxylin-eosin (HE), elastica van Gieson (EVG; for collagen), or α-SMA. The extent of fibroproliferation and scar formation in sections was evaluated in a blinded manner.

Statistical Analysis

Data are presented as the mean ± SEM. Statistical comparisons of multiple groups used one-way or two-way repeated-measures analysis of variance (ANOVA) followed by the Bonferroni/Dunn post hoc test. Comparisons of two groups used Student's *t*-test with Bonferroni correction. Differences were considered statistically significant at $P < 0.05$.

Results

Toxicology of Y-27632: Effects on HTFs

The result of the trypan blue exclusion test showed that the percentage of living HTFs was 96.4% ± 0.3% in control cultures without Y-27632 treatment. In experimental cultures treated with various concentrations of Y-27632, percentages of living cells were 96.7% ± 0.4%, 97.3% ± 0.5%, and 96.5 ± 0.4 for 1, 10, and 100 μM Y-27632, respectively. These values were not significantly different from the control value.

Cell proliferation was measured by the MTT assay. The assay is based on measuring the intracellular formazan spectrophotometrically which is facilitated by active cells. The optical absorbance of Y-27632-treated cells were 0.66 ± 0.02, 0.66 ± 0.02, and 0.67 ± 0.01 for 1, 10, and 100 μM Y-27632 respectively, while that of control cells was 0.67 ± 0.03. The MTT assay revealed no significant differences between Y-27632-treated HTFs and control samples. This inhibitor thus displayed little toxicity and had no effect on proliferative activity of HTFs.

Influence of Y-27632 on Adhesion of HTFs to the ECM

Compared with controls, greater numbers of Y-27632-treated HTFs adhered to fibronectin and collagen type I, with adhesion to both fibronectin and collagen showing a Y-27632 concentration-dependent effect (Fig. 1). Results were statistically significant for both fibronectin (at 10 μM) and collagen type I (at 100 μM).

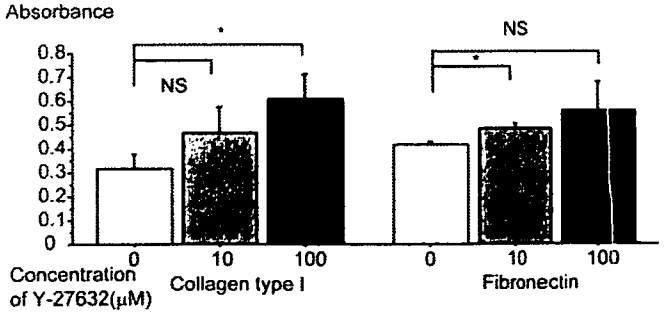

FIGURE 1. Effect of Y-27632 on adhesion of HTFs. To elucidate interactions between cultured HTFs and ECM components, adhesion of HTFs to fibronectin-coated or collagen type I–coated dishes was investigated. The cells were plated on dishes coated with fibronectin (10 μg/mL) or collagen type I (0.5 μg/mL) and were allowed to adhere in the absence or presence of 10 or 100 μM Y-27632 for 60 minutes. Adherence was measured by means of the calcein-AM assay. The relative remaining number of cells was determined based on optical absorbance of fluorescence with an emission wavelength of 520 nm measured by an automated plate reader. Data are expressed as the mean ± SEM ($n = 6$). *$P < 0.05$ versus control.

Effects of Y-27632 on the Cytoskeleton and on α-SMA Expression

In an immunohistochemical study, LPA treatment induced assembly of actin stress fibers and increased the number of focal adhesions in HTFs. Addition of Y-27632 prevented this assembly and focal adhesion expression (Figs. 2A, 2B). Addition of LPA, however, caused redistribution of focal adhesions in the cell periphery. (Fig. 2B).

HTFs were stimulated with LPA in the presence of 10 μM Y-27632 or vehicle control. Although untreated serum-starved cells showed weak α-SMA staining, LPA treatment induced assembly of α-SMA-positive stress fibers in approximately 50% of the cells, and addition of Y-27632 prevented these LPA-induced effects (Fig. 2C).

Gel Contraction Assay

Compared with controls, Y-27632 caused significant concentration-dependent inhibition of HTF-mediated collagen gel contraction in the presence of serum (Fig. 3A). At 48 hours after plating and incubation without Y-27632, the original diameter of the gels (16 mm) changed to 5.5 ± 0.2 mm ($n = 4$). However, with addition of 1, 10, or 100 μM Y-27632, collagen gel diameters at the same time point measured 4.4 ± 0.4, 1.9 ± 0.2, and 0.4 ± 0.2 mm, respectively (Fig. 3B). Experiments at 72 and 96 hours produced similar results. Results were statistically significant, and dose dependency was evident ($P < 0.001$).

HTF Cell Motility Activities

At 9 hours after the scraping, the distance between the edges of the exposed regions was 71.7% ± 4.4%, 51.2% ± 3.6%, 24.9% ± 3.0%, 7.6 ± 2.8% respectively, with Y-27632 at 0 (control), 1, 10, and 100 μM (Fig. 4). The increase in Y-27632-induced wound healing was significant and depended on concentration.

Effects of Y-27632 on Filtration Blebs

Topical instillation of Y-27632 significantly improved the results of glaucoma filtration surgery in this rabbit model and prolonged bleb survival compared with vehicle-treated control animals. Figure 5A shows the typical appearance of the blebs during the 7 postoperative days. Slit lamp examination showed that the treatment with Y-27632 was associated with elevated, diffuse blebs with mild conjunctival injection rather than the flat, scarred, vascularized blebs in the controls. In the vehicle-treated controls, vascularization in the conjunctiva was significant. Although no significant differences in anterior chamber depth or anterior chamber inflammation were observed between Y-27632-treated and control groups, postoperative IOP was significantly lower in the Y-27632-treated group (Fig. 5B). No significant postoperative changes in pupil dilation or cornea were observed in both groups. Analysis of bleb scores revealed significant differences between the Y-27632-treated and vehicle-treated control groups (Fig. 5C).

Effects of Y-27632 on Histologic Characteristics of Eyes in a Rabbit Model of Glaucoma Filtration Surgery

Surgical sites were examined 7 days after the surgery and stained with HE, EVG, or α-SMA. HE stain of vehicle-treated eyes exhibited nearly complete scarring over the sclerostomy site (Fig. 6A), including evidence of new collagen deposition in the scleral gap and bleb area, as shown by EVG stain (Fig. 6C).

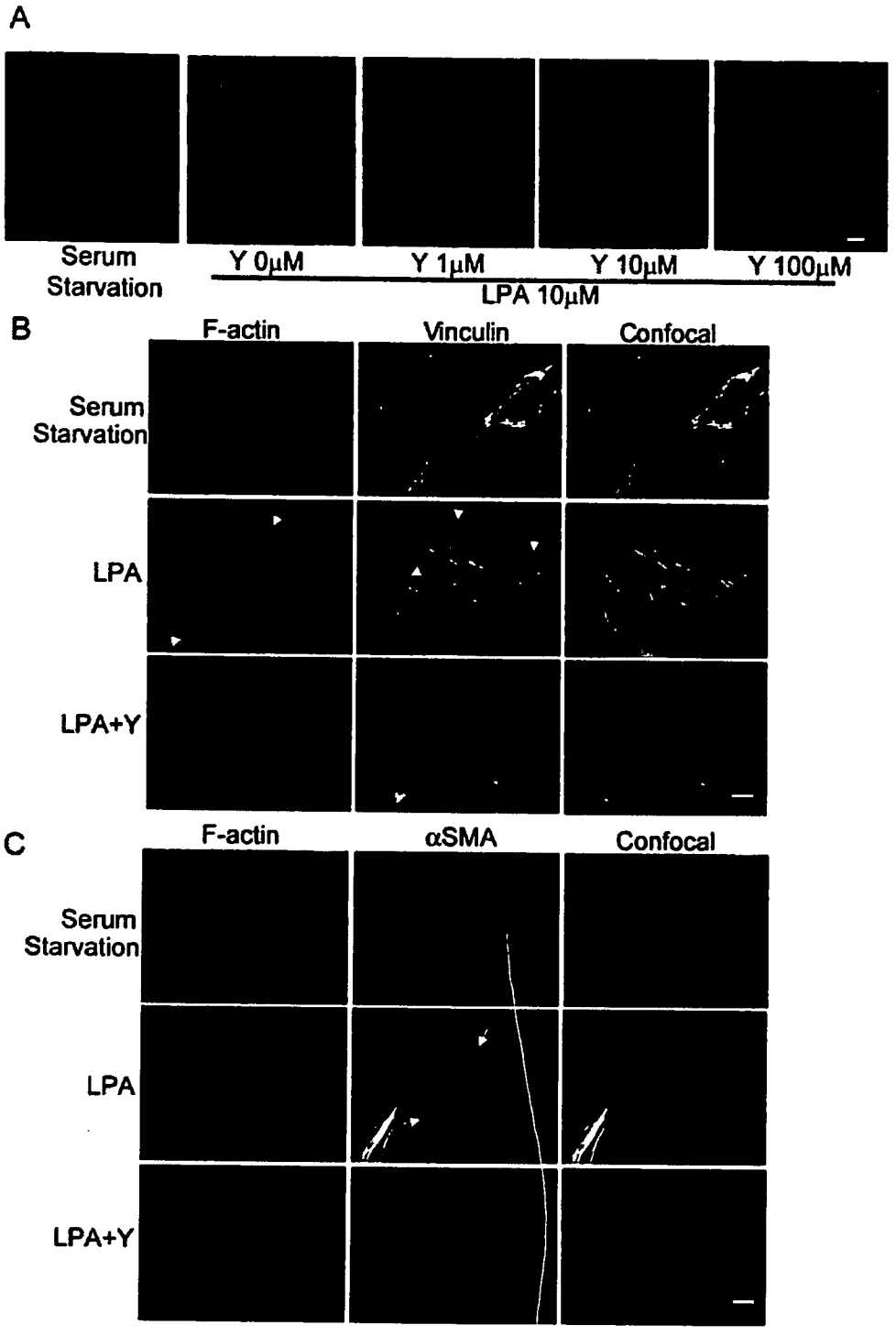

FIGURE 2. Effect of Y-27632 on the cytoskeleton and on α-SMA expression. (A) Distribution of F-actin in HTFs. Serum-starved HTFs were incubated with 10 μM LPA for 10 minutes and were then incubated without (control, 0 μM) or with 1, 10, or 100 μM Y-27632 for 30 minutes. Experiments repeated three times yielded similar results. (B) Distribution of F-actin and vinculin in HTFs. Serum-starved HTFs were stimulated with 10 μM LPA for 10 minutes and were then incubated with 10 μM Y-27632 for 30 minutes. LPA induced assembly of actin stress fibers (B, *white arrows*) and redistribution of focal adhesions in the cell periphery (B, *white arrowheads*), and Y-27632 prevented these effects. *Right*: merged images. (C) Distribution of F-actin and α-SMA in HTFs. α-SMA expression is a hallmark of myofibroblast generation and the cells' fibrogenic reaction. The cells were stimulated with LPA in the presence of 10 μM Y-27632. LPA treatment induced assembly of α-SMA-positive stress fibers (C, *white arrows*). Y-27632 prevented LPA-induced expression of α-SMA and its incorporation into actin stress fibers. *Right*: merged images. Scale bars, 50 μm.

In contrast, HE stain showed that postoperative scar formation at day 7 was significantly reduced by Y-27632 treatment (Fig. 6B). EVG stain showed that eyes treated with Y-27632 had bleb cavities of moderate size and evidence of minimal deposition of new collagen in the sclera (Fig. 6D). As judged by EVG with higher magnification, both the conjunctiva and the subconjunctival scar (Fig. 6E) and the area around the failed bleb (Fig. 6G) in the vehicle-treated group consisted of dense collagen fibers and scar tissue. In contrast, the surviving Y-27632-treated bleb showed a much looser architecture with a visible conjunctiva (Fig. 6F) and bleb formation with fewer collagen deposits (Fig. 6H). The sclerostomy area in the vehicle-treated eye consisted of densely packed collagen (Fig. 6I), whereas the site in the Y-27632-treated group differed and showed loose cell infiltration without significant collagen deposition (Fig. 6J). At the microscopic level, no significant changes in the trabecular meshwork were observed after Y-27632-treatment compared with the vehicle-treated group.

Immunohistochemical staining of blebs on postoperative day 7 demonstrated reduced expression of α-SMA after Y-27632 treatment (Fig. 6K) compared with the control (Fig. 6L).

DISCUSSION

Scarring is a major reason for failure of filtration surgery. Several studies showed that subconjunctival scarring of the

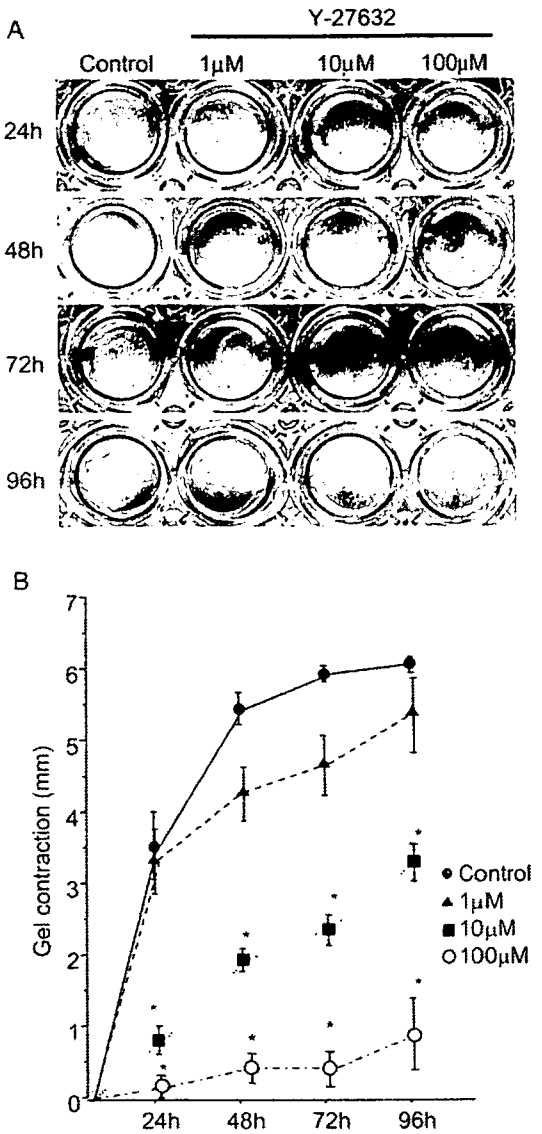

FIGURE 3. Effects of Y-27632 on HTF-mediated collagen gel contraction. (A) Collagen gels were incubated without (Control) or with Y-27632 (1, 10, or 100 μM) for up to 96 hours. (B) The extent of contraction of collagen gels mediated by HTFs was expressed as the decrease in gel diameter compared with the initial diameter. Changes in diameters of collagen gels in the absence (control) or presence of Y-27632 at 1, 10, or 100 μM were measured. Data are shown as the mean ± SEM (n =4). $P < 0.001$ versus control. Compared with the control, Y-27632 caused statistically significant, concentration-dependent inhibition of HTF-mediated collagen gel contraction ($P < 0.001$).

filtering bleb site is mainly mediated by HTF proliferation, migration, and contraction.[28-30] Fibroblasts, including HTFs,[21] are stimulated by growth factors to differentiate into myofibroblasts both in vitro[31-33] and in vivo.[34] Myofibroblasts are responsible for fibrosis via increased ECM synthesis, for granulation tissue formation, and wound contraction.[35,36]

The use of antimetabolites has been one of the most important developments in glaucoma surgery.[37,38] However, antimetabolite treatment can result in several postoperative bleb-related problems.[1,39,40] Therefore, alternative anti-scarring agents that do not cause extensive tissue damage are needed. In the present study, a specific ROCK inhibitor, Y-27632, induced profound changes in cultured HTFs without significant toxicity or inhibition of HTF proliferation. In addition, topical instillation of Y-27632 was highly effective in reducing scar tissue formation in a rabbit model of glaucoma filtration surgery.

Our in vitro results revealed that exposure to Y-27632 enhanced adhesiveness of cells to the ECM. This finding correlates well with our previous report on TM cells.[19] The actin cytoskeleton is known to interact with integrins to regulate cell shape and adhesiveness of cells to the ECM. Y-27632 reportedly promotes integrin adhesion in cultured THP-1 monocytes.[41] Our immunocytochemical investigation in the present study documented redistribution of focal adhesions in the cell periphery (Fig. 4B). This increased adhesiveness of cells to the ECM may be related to alterations in cell shape and redistribution of focal adhesions to the cell periphery.

LPA, a bioactive lipid growth factor that is present in aqueous humor, regulates various cellular events.[42] LPA, associated with activation of the Rho, induces very strong actin fibers and focal adhesions in various kinds of cells. A previous study of myofibroblasts demonstrated that LPA and serum, as well as TGF-β, could activate myofibroblast differentiation.[43,44] which is supposedly one of the most potent stimulators of HTFs.[29] After glaucoma filtration surgery, HTFs are likely to be exposed to LPA via serum and/or plasma, because the blood-aqueous humor barrier breaks down, and circulating aqueous humor bathes the wound site.[45] Y-27632 has been reported to inhibit LPA-promoted myofibroblast contraction in the collagen lattice model, which suggests that contraction depends on activation of the Rho.[46-48] In the present study, we investigated LPA-induced α-SMA expression in HTFs to analyze the direct role of the Rho signaling pathway in these cells. Treatment with Y-27632 reduced LPA-induced α-SMA expression in HTFs, which suggests that Y-27632 functions as a potent antiscarring agent via inhibition of transdifferentiation of HTFs into myofibroblasts.

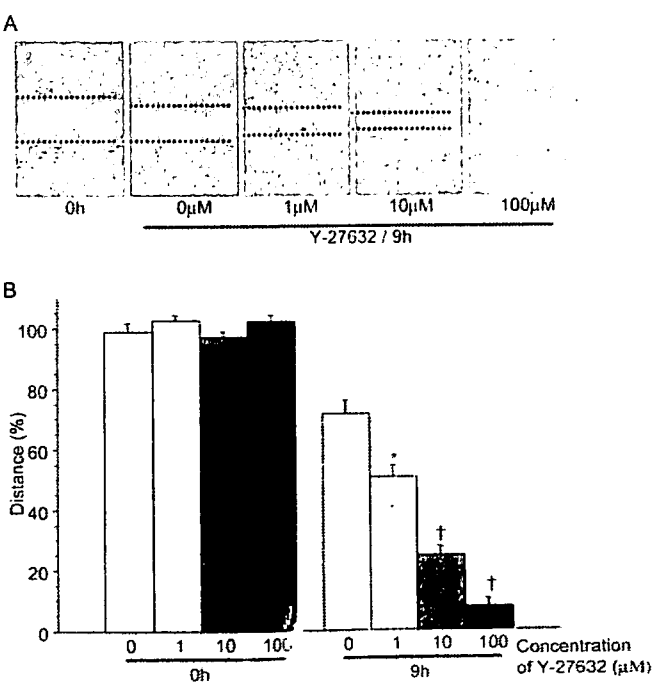

FIGURE 4. Effects of Y-27632 on cell motility activities of HTFs. (A) Confluent cultures were scraped with a yellow pipette tip to create a cell-free linear wound. Medium was replaced with fresh medium without (control) or with Y-27632 (1, 10, or 100 μM). After 9 hours, migration of cells into the wound area was photographed. *Dotted lines*: edges of the migrated cells. (B) Distances between edges of migrated cells were measured and are shown as the mean ± SEM (n = 6); the distance before treatment was set at 100%. $^*P < 0.05$, $\dagger P < 0.001$ versus control.

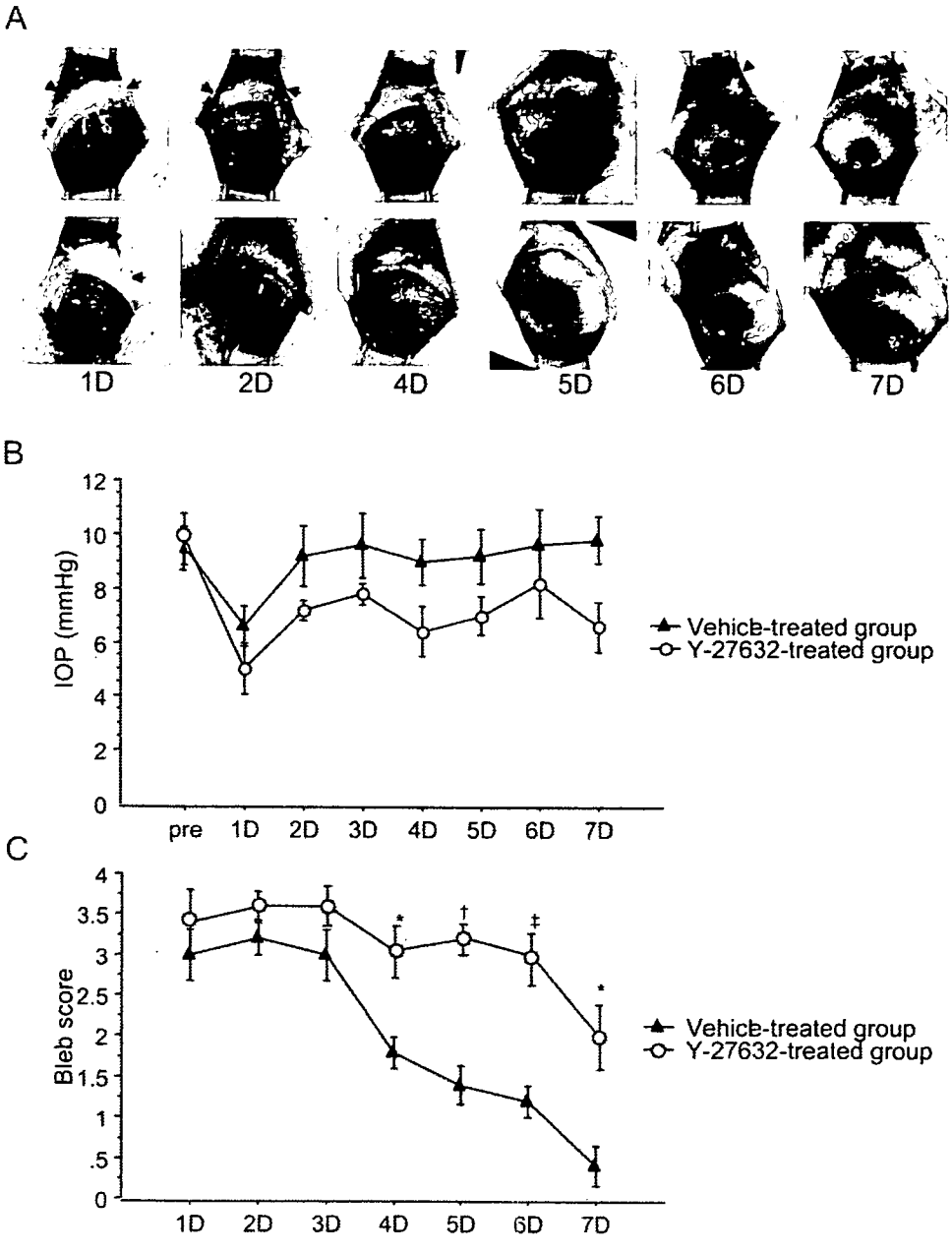

FIGURE 5. Postoperative IOP, bleb features, and bleb scores. (A) Representative postoperative photographs show surviving conjunctival blebs in the Y-27632-treated group that remained diffusely elevated (*top*). A flat, scarred, vascularized bleb, formed after vehicle treatment, is an example of a bleb that did not survive (*bottom*). *Arrows*: edges of the blebs. (B) Postoperative IOP changes in the two groups showed significance between the Y-27632-treated group and the vehicle-treated group 7 days ($P < 0.05$) after surgery. (C) Bleb scores for rabbit eyes treated with Y-27632 or vehicle. The mean ± SEM for six eyes for each treatment is shown for 7 postoperative days. Y-27632-treated eyes exhibited significantly higher bleb scores compared with the control during the 7 days ($P < 0.001$). Y-27632-treated eyes exhibited significantly higher bleb scores compared with the control from days 4 to 7. (*$P < 0.05$, †$P < 0.001$, ‡$P < 0.005$ versus control.)

Gel contraction experiments using three-dimensional cultures of HTFs embedded in collagen type I gels revealed that addition of Y-27632 decreased contraction of gels. This result suggests reduced cell contractility and/or altered interaction between HTFs and collagen type I. Y-27632 treatment increased cell adhesion to collagen type I, and so the change in gel contraction is thought to be due to the relaxation of the HTFs induced by Y-27632.

Our results indicate that administration of Y-27632 enhanced the motility of the HTFs, which is in agreement with the idea that stabilization of actin stress fibers limits cell movement. We have reported that Y-27632 enhances motility of cultured TM cells.[19] In the same study, we demonstrated reduced levels of phosphorylated LIM kinase 2 and cofilin, which is one of the targets downstream of Rho signaling pathways. A previous report from other laboratories showed that constitutively active RhoAV14 significantly inhibited wound closure and that incubation with Y-27632 promotes wound healing.[20] As shown by others[49,50] and according to findings in the present study, inhibition of formation of stress fibers and focal adhesions via Y-27632 improves cell migration during wound healing. Several candidate antiscarring agents, such as alkylphosphocholines and p38 inhibitors, are also reported to inhibit HTF proliferation and contraction.[3,4] Although alkylphosphocholines are reported to inhibit migration of HTFs,[3] the main effect of p38 inhibitors is supposed to be an inhibition of transdifferentiation of HTFs into myofibroblasts.[4] In contrast, it is interesting that we found that Y-27632 not only increased migration but also inhibited cell contraction and transdifferentiation of HTFs into myofibroblasts. These findings, taken together, suggest that inhibition of migration may not be necessary for antiscarring effects when associated with decreased myofibroblast transdifferentiation and inhibited cell contraction. However, further studies are needed to elucidate the association of migration and scar formation after Y-27632 treatment.

In an animal model of filtration surgery, obstruction of the sclerostomy site from excessive ECM deposition and contrac-

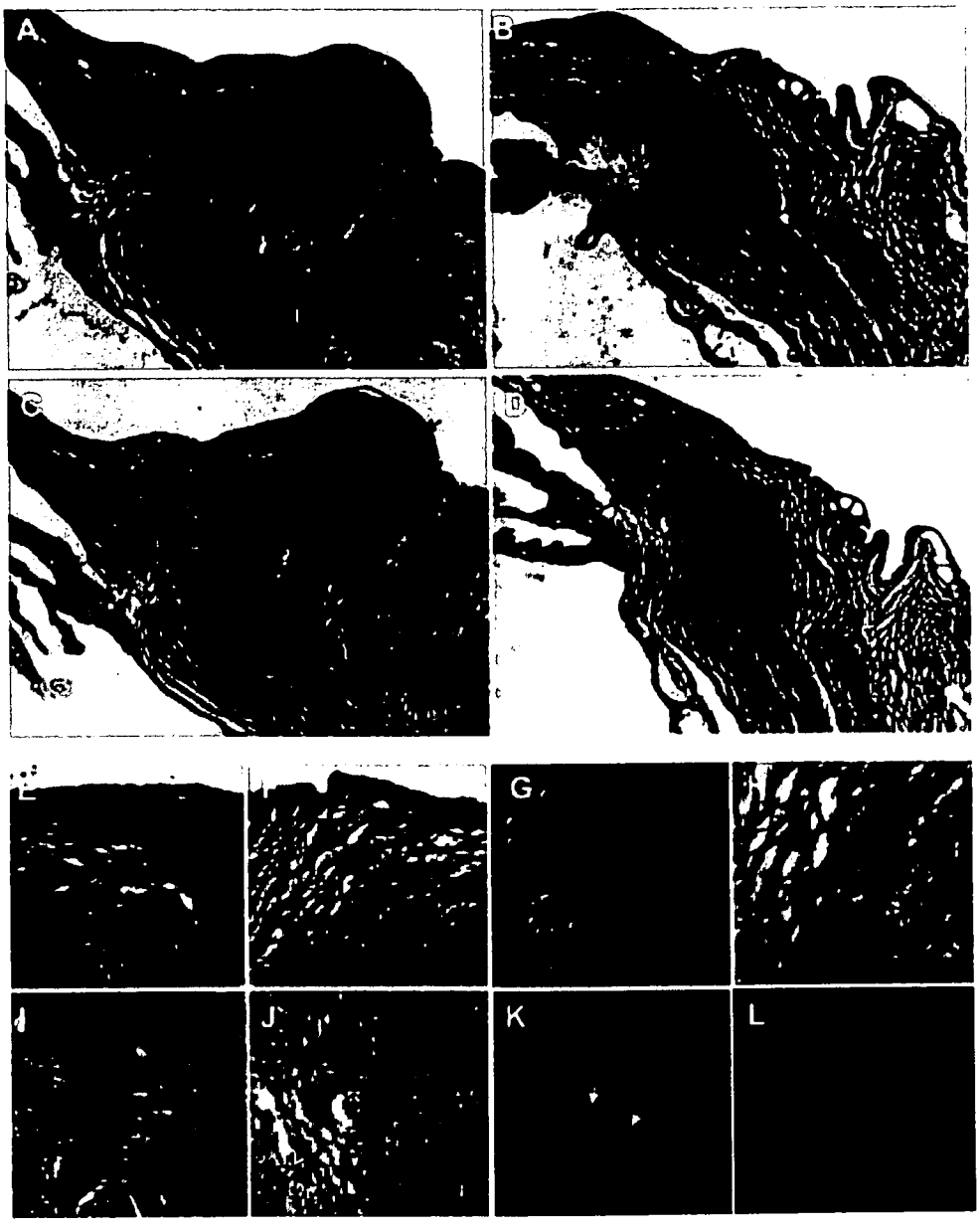

FIGURE 6. Histologic characteristics of postoperative blebs. Y-27632 treatment reduced scarring at the microscopic level. The images show representative sections from eyes in each group. HE stain revealed that the total amount of scar tissue in the subconjunctival space was significantly greater in vehicle-treated (A) than in Y-27632-treated (B) eyes at day 7. EVG stain revealed that vehicle-treated eyes contained scar tissue with densely packed collagen deposits (C, *arrows*) and that the size of the collagen deposits was significantly greater than that in Y-27632-treated eyes (D, *arrows*). EVG also showed that subconjunctival scarring in a vehicle-treated failed bleb consisted of dense collagen fibers and fibroblasts (E, *arrows*) and that the failed bleb area was densely packed with collagen deposits and fibroblasts (G). In contrast, the surviving Y-27632-treated bleb showed much looser architecture with a visible conjunctiva (F) and bleb formation with less collagen (H). In the area of sclerostomy, the wound site of the failed vehicle-treated bleb consisted of densely packed collagen (I, *arrows*). The sclerostomy site in the Y-27632-treated group, different from that in the vehicle-treated group, showed loose cell infiltration without significant collagen deposition (J). Immunohistochemical staining for α-SMA in postoperative blebs on day 7 demonstrated reduced α-SMA expression after Y-27632 treatment (L) compared with massive α-SMA expression of the control eye (K, *white arrows*). Magnification: (A–D) ×25; (E, F, K, L) ×100; (G–J) ×200.

tion due to transdifferentiation of fibroblasts into myofibroblasts, which is characterized by synthesis of α-SMA, have been reported.[51,52] In our present study, histologic analysis of rabbit tissues showed that topical instillation of Y-27632 significantly reduced subconjunctival collagen deposition compared with controls. Y-27632 also significantly reduced the population of cells expressing α-SMA, which indicates inhibition of myofibroblast transdifferentiation in vivo. These observations are in good agreement with the present in vitro data that Y-27632 significantly reduced α-SMA expression in HTFs, suggesting that beneficial effects of Y-27632 in glaucoma surgery may be mediated by reduced cell contraction and inhibition of transdifferentiation of fibroblasts.

Previously, we have reported the significant IOP-lowering effects of ROCK inhibitors and have shown the possibilities for clinical use.[18,53] We have already conducted a phase I clinical trial for the ROCK inhibitor as an IOP-lowering agent and have demonstrated its safety and effectiveness.[54] The present study showed that ROCK inhibitors may have beneficial effects, not only for IOP-lowering but also for bleb formation after filtering surgery. However, further studies are needed to determine the optimal dosage for antiscarring effects. In addition, no direct comparisons were made with effects of MMC. Therefore, we are currently performing a comparison of surgical outcomes for use of Y-27632 and MMC.

In conclusion, our results indicate that Y-27632, a selective ROCK inhibitor, effectively reduced subconjunctival scarring after experimental glaucoma filtration surgery. Y-27632 was safe and well tolerated in this model. Further study is needed to determine whether inhibition of the ROCK/ROK family can lead to development of an alternative, more physiological agent to protect against postoperative scarring.

References

1. Yoon PS, Singh K. Update on antifibrotic use in glaucoma surgery, including use in trabeculectomy and glaucoma drainage implants and combined cataract and glaucoma surgery. *Curr Opin Ophthalmol.* 2004;15:141–146.
2. Mead AL, Wong TT, Cordeiro MF, Anderson IK, Khaw PT. Evaluation of anti-TGF-β2 antibody as a new postoperative anti-scarring agent in glaucoma surgery. *Invest Ophthalmol Vis Sci.* 2003;44:3394–3401.

3. Eibl KH, Banas B, Kook D, et al. Alkylphosphocholines: a new therapeutic option in glaucoma filtration surgery. *Invest Ophthalmol Vis Sci.* 2004;45:2619-2624.
4. Meyer-ter-Vehn T, Gebhardt S, Sebald W, et al. p38 inhibitors prevent TGF-β-induced myofibroblast transdifferentiation in human tenon fibroblasts. *Invest Ophthalmol Vis Sci.* 2006;47:1500-1509.
5. Ehrlich HP, Rajaratnam JB. Cell locomotion forces versus cell contraction forces for collagen lattice contraction: an in vitro model of wound contraction. *Tissue Cell.* 1990;22:407-417.
6. Tomasek JJ, Gabbiani G, Hinz B, Chaponnier C, Brown RA. Myofibroblasts and mechano-regulation of connective tissue remodelling. *Nat Rev Mol Cell Biol.* 2002;3:349-363.
7. Hinz B, Mastrangelo D, Iselin CE, Chaponnier C, Gabbiani G. Mechanical tension controls granulation tissue contractile activity and myofibroblast differentiation. *Am J Pathol.* 2001;159:1009-1020.
8. Desmouliere A, Chaponnier C, Gabbiani G. Tissue repair, contraction, and the myofibroblast. *Wound Repair Regen.* 2005;13:7-12.
9. Morishige K, Shimokawa H, Eto Y, et al. Adenovirus-mediated transfer of dominant-negative rho-kinase induces a regression of coronary arteriosclerosis in pigs in vivo. *Arterioscler Thromb Vasc Biol.* 2001;21:548-554.
10. Kaibuchi K, Kuroda S, Amano M. Regulation of the cytoskeleton and cell adhesion by the Rho family GTPases in mammalian cells. *Annu Rev Biochem.* 1999;68:459-486.
11. Somlyo AP, Somlyo AV. Signal transduction by G-proteins, rho-kinase and protein phosphatase to smooth muscle and non-muscle myosin II. *J Physiol.* 2000;522:177-185.
12. Fukata Y, Amano M, Kaibuchi K. Rho-Rho-kinase pathway in smooth muscle contraction and cytoskeletal reorganization of non-muscle cells. *Trends Pharmacol Sci.* 2001;22:32-39.
13. Hall A. Rho GTPases and the actin cytoskeleton. *Science.* 1998;279:509-514.
14. Ridley AJ. Rho GTPases and cell migration. *J Cell Sci.* 2001;114:2713-2722.
15. Ishizaki T, Maekawa M, Fujisawa K, et al. The small GTP-binding protein Rho binds to and activates a 160 kDa Ser/Thr protein kinase homologous to myotonic dystrophy kinase. *EMBO J.* 1996;15:1885-1893.
16. Nakagawa O, Fujisawa K, Ishizaki T, Saito Y, Nakao K, Narumiya S. ROCK-I and ROCK-II, two isoforms of Rho-associated coiled-coil forming protein serine/threonine kinase in mice. *FEBS Lett.* 1996;392:189-193.
17. Riento K, Ridley AJ. Rocks: multifunctional kinases in cell behaviour. *Nat Rev Mol Cell Biol.* 2003;4:446-456.
18. Honjo M, Tanihara H, Inatani M, et al. Effects of rho-associated protein kinase inhibitor Y-27632 on intraocular pressure and outflow facility. *Invest Ophthalmol Vis Sci.* 2001;42:137-144.
19. Koga T, Awai M, Tsutsui J, Yue BY, Tanihara H. Rho-associated protein kinase inhibitor, Y-27632, induces alterations in adhesion, contraction and motility in cultured human trabecular meshwork cells. *Exp Eye Res.* 2006;82:362-370.
20. Nobes CD, Hall A. Rho GTPases control polarity, protrusion, and adhesion during cell movement. *J Cell Biol.* 1999;144:1235-1244.
21. Meyer-ter-Vehn T, Sieprath S, Katzenberger B, Gebhardt S, Grehn F, Schlunck G. Contractility as a prerequisite for TGF-β-induced myofibroblast transdifferentiation in human tenon fibroblasts. *Invest Ophthalmol Vis Sci.* 2006;47:4895-4904.
22. Jain PT, Pento JT, Graves DC. Cell-growth quantitation methods for the evaluation of antiestrogens in human breast cancer cells in culture. *J Pharmacol Toxicol Methods.* 1992;27:203-207.
23. Zhou L, Zhang SR, Yue BY. Adhesion of human trabecular meshwork cells to extracellular matrix proteins: roles and distribution of integrin receptors. *Invest Ophthalmol Vis Sci.* 1996;37:104-113.
24. Nakamura Y, Hirano S, Suzuki K, Seki K, Sagara T, Nishida T. Signaling mechanism of TGF-β1-induced collagen contraction mediated by bovine trabecular meshwork cells. *Invest Ophthalmol Vis Sci.* 2002;43:3465-3472.
25. Nakamura Y, Sagara T, Seki K, Hirano S, Nishida T. Permissive effect of fibronectin on collagen gel contraction mediated by bovine trabecular meshwork cells. *Invest Ophthalmol Vis Sci.* 2003;44:4331-4336.
26. Yamanaka O, Saika S, Okada Y, Ooshima A, Ohnishi Y. Effects of interferon-γ on human subconjunctival fibroblasts in the presence of TGFβ1: reversal of TGFβ-stimulated collagen production. *Graefes Arch Clin Exp Ophthalmol.* 2003;241:116-124.
27. Perkins TW, Faha B, Ni M, et al. Adenovirus-mediated gene therapy using human p21WAF-1/Cip-1 to prevent wound healing in a rabbit model of glaucoma filtration surgery. *Arch Ophthalmol.* 2002;120:941-949.
28. Migdal C, Gregory W, Hitchings R. Long-term functional outcome after early surgery compared with laser and medicine in open-angle glaucoma. *Ophthalmology.* 1994:101:1651-1656; discussion 1657.
29. Khaw PT, Occleston NL, Schultz G, Grierson I, Sherwood MB, Larkin G. Activation and suppression of fibroblast function. *Eye.* 1994;8:188-195.
30. Occleston NL, Daniels JT, Tarnuzzer RW, et al. Single exposures to antiproliferatives: long-term effects on ocular fibroblast wound-healing behavior. *Invest Ophthalmol Vis Sci.* 1997;38:1998-2007.
31. Desmouliere A, Geinoz A, Gabbiani F, Gabbiani G. Transforming growth factor-b1 induces α-smooth muscle actin expression in granulation tissue myofibroblasts and in quiescent and growing cultured fibroblasts. *J Cell Biol.* 1993;122:103-111.
32. Grotendorst GR. Connective tissue growth factor: a mediator of TGF-β action on fibroblasts. *Cytokine Growth Factor Rev.* 1997;8:171-179.
33. Leask A, Abraham DJ. TGF-β signaling and the fibrotic response. *FASEB J.* 2004;18:816-827.
34. Sime PJ, Xing Z, Graham FL, Csaky KG, Gauldie J. Adenovector-mediated gene transfer of active transforming growth factor-b1 induces prolonged severe fibrosis in rat lung. *J Clin Invest.* 1997;100:768-776.
35. Gabbiani G, Ryan GB, Majne G. Presence of modified fibroblasts in granulation tissue and their possible role in wound contraction. *Experientia.* 1971;27:549-550.
36. Skalli O, Ropraz P, Trzeciak A, Benzonana G, Gillessen D, Gabbiani G. A monoclonal antibody against alpha-smooth muscle actin: a new probe for smooth muscle differentiation. *J Cell Biol.* 1986;103:2787-2796.
37. Khaw PT, Ward S, Porter A, Grierson I, Hitchings RA, Rice NS. The long-term effects of 5-fluorouracil and sodium butyrate on human Tenon's fibroblasts. *Invest Ophthalmol Vis Sci.* 1992;33:2043-2052.
38. Khaw PT, Doyle JW, Sherwood MB, Smith MF, McGorray S. Effects of intraoperative 5-fluorouracil or mitomycin C on glaucoma filtration surgery in the rabbit. *Ophthalmology.* 1993;100:367-372.
39. Mac I, Soltau JB. Glaucoma-filtering bleb infections. *Curr Opin Ophthalmol.* 2003;14:91-94.
40. Anand N, Arora S, Clowes M. Mitomycin C augmented glaucoma surgery: evolution of filtering bleb avascularity, transconjunctival oozing, and leaks. *Br J Ophthalmol.* 2006;90:175-180.
41. Worthylake RA, Burridge K. RhoA and ROCK promote migration by limiting membrane protrusions. *J Biol Chem.* 2003;278:13578-13584.
42. Hla T, Lee MJ, Ancellin N, Paik JH, Kluk MJ. Lysophospholipids: receptor revelations. *Science.* 2001;294:1875-1878.
43. Yin Z, Watsky MA. Chloride channel activity in human lung fibroblasts and myofibroblasts. *Am J Physiol.* 2005;288:L1110-L1116.
44. Watsky MA. Lysophosphatidic acid, serum, and hyposmolarity activate Cl- currents in corneal keratocytes. *Am J Physiol.* 1995;269:C1385-C1393.
45. Wong TT, Mead AL, Khaw PT. Matrix metalloproteinase inhibition modulates postoperative scarring after experimental glaucoma filtration surgery. *Invest Ophthalmol Vis Sci.* 2003;44:1097-1103.
46. Tomasek JJ, Vaughan MB, Kropp BP, et al. Contraction of myofibroblasts in granulation tissue is dependent on Rho/Rho kinase/myosin light chain phosphatase activity. *Wound Repair Regen.* 2006;14:313-320.
47. Parizi M, Howard EW, Tomasek JJ. Regulation of LPA-promoted myofibroblast contraction: role of Rho, myosin light chain kinase, and myosin light chain phosphatase. *Exp Cell Res.* 2000;254:210-220.

48. Tangkijvanich P, Melton AC, Santiskulvong C, Yee HF Jr. Rho and p38 MAP kinase signaling pathways mediate LPA-stimulated hepatic myofibroblast migration. *J Biomed Sci.* 2003;10:352–358.
49. Narumiya S, Ishizaki T, Watanabe N. Rho effectors and reorganization of actin cytoskeleton. *FEBS Lett.* 1997;410:68–72.
50. Amano M, Fukata Y, Kaibuchi K. Regulation and functions of Rho-associated kinase. *Exp Cell Res.* 2000;261:44–51.
51. Darby IA, Hewitson TD. Fibroblast differentiation in wound healing and fibrosis. *Int Rev Cytol.* 2007;257:143–179.
52. Miller MH, Grierson I, Unger WI, Hitchings RA. Wound healing in an animal model of glaucoma fistulizing surgery in the rabbit. *Ophthalmic Surg.* 1989;20:350–357.
53. Tokushige H, Inatani M, Nemoto S, et al. Effects of topical administration of y-39983, a selective Rho-associated protein kinase inhibitor, on ocular tissues in rabbits and monkeys. *Invest Ophthalmol Vis Sci.* 2007;48:3216–3222.
54. Tanihara H, Inatani M, Honjo M, et al. Intraocular pressure lowering effects and safety of topical administration of a selective ROCK inhibitor, SNJ-1656, in normal volunteers. *Arch Ophthalmol.* In press.

Current Eye Research, 32:991–997, 2007
Copyright © Informa Healthcare USA, Inc.
ISSN: 0271-3683 print / 1460-2202 online
DOI: 10.1080/02713680701649603

informa
healthcare

Pitavastatin: Protection against Neuronal Retinal Damage Induced by Ischemia-Reperfusion Injury in Rats

Takahiro Kawaji, Yasuya Inomata, Akiomi Takano, Nina Sagara, Masaru Inatani, Mikiko Fukushima, and Hidenobu Tanihara
Department of Ophthalmology and Visual Science, Graduate School of Medical Sciences, Kumamoto University, Honjo, Kumamoto, Japan

Megumi Honjo
Department of Ophthalmology, Kitano Hospital, Ogimachi, Kita-ku, Osaka, Japan

ABSTRACT *Purpose*: To evaluate the neuroprotective effects of pitavastatin against neuronal retinal damage induced by ischemia-reperfusion injury in rats. *Methods and Results*: Ischemia-reperfusion injury was induced in Sprague-Dawley rats using ocular hypertension. Pitavastatin (0.1, 0.5, or 1.0 mg/kg) was given intravenously 12 hr or 5 min before, or 12 or 24 hr after the induction of ischemia-reperfusion injury. Morphometric and retrograde labeling analyses revealed neuroprotective effects when pitavastatin (0.5 mg/kg) was administered 5 min before–even 12 and 24 hr–after induction of ischemia-reperfusion injury. These effects depended on dose; protection was noted at pitavastatin concentrations of 0.5 and 1 mg/kg but not 0.1 mg/kg. Furthermore, preadministration of pitavastatin (0.5 mg/kg) reduced expression of P-selectin and intercellular adhesion molecule-1 at 12 and 24 hr after induction of ischemia-reperfusion injury. *Conclusions*: As pitavastatin was efficacious in preventing retinal neuronal death, it may be a novel therapeutic modality for ischemic retinal diseases.

KEYWORDS ischemia-reperfusion injury; ischemic retinal disease; neuroprotection; pitavastatin

INTRODUCTION

Statins, which are 3-hydroxy-3-methylglutaryl coenzyme A (HMG-CoA) reductase inhibitors, have gained wide acceptance as important agents for treatment of hypercholesterolemia. These inhibitors exert biological effects by blocking conversion of HMG-CoA to mevalonate. Clinical studies of statins have also reported a lower incidence of cerebrovascular and cardiovascular disease independent of the ability of statins to reduce low-density lipoprotein cholesterol levels.[1–5]

The association between the use of statins and vision-threatening diseases, such as age-related macular degeneration (AMD) and diabetic retinopathy, has been evaluated in many clinical and experimental studies; however, the results have been contradictory.[6–14] We previously reported that improvement of endothelial function via the pleiotropic actions of two statins, pravastatin and cerivastatin, could aid in the protection of retinal neurons against damage resulting from ischemic retina.[11] Simvastatin was also reportedly beneficial in inhibition of leukocyte accumulation and vascular permeability in the retina

Received 13 June 2007
Accepted 24 August 2007

Correspondence: Takahiro Kawaji, MD, Ph.D., Department of Ophthalmology and Visual Science, Graduate School of Medical Sciences, Kumamoto University, 1-1-1 Honjo, Kumamoto 860-8556, Japan. E-mail: kawag@white.plala.or.jp

in a rat model of diabetes.[14] These data suggest the potential of statins to be important drugs for treatment of ischemic retinal diseases.

We report here the neuroprotective effects of pitavastatin (so-called vascular statin), which has a high affinity for vascular endothelium against neuronal retinal damage induced by ischemia-reperfusion injury in rats.

MATERIALS AND METHODS

Animals and Model of Ischemia

Male Sprague-Dawley rats (200–250 g) were used in this study. All experiments were performed in accordance with the Statement for the Use of Animals in Ophthalmic and Visual Research of the Association for Research in Vision and Ophthalmology.

Transient ocular hypertension was induced in the right eye of each rat, according to the method of Rosenbaum et al.,[15] with slight modifications. Rats were anesthetized with a 1:1 mixture of xylazine hydrochloride (4 mg/kg) and ketamine hydrochloride (10 mg/kg). Dilation of the pupil was achieved with 0.5% tropicamide and 2.5% phenylephrine hydrochloride. The anterior chamber of the right eye was cannulated with a 30-gauge needle attached to a line for infusion of balanced salt solution. Intraocular pressure (IOP) was raised to 130 mmHg. Complete non-perfusion was confirmed via an operating microscope. After 60 min of ocular hypertension, the needle was withdrawn and the IOP normalized. The operating microscope was also used to verify reperfusion of the vessels.

Chemicals and Drug Administration

Pitavastatin (trade name: Livalo, code name: NK-104) was generously provided by Kowa (Nagoya, Japan). Carboxymethyl cellulose (CMC) sodium salt, which served as the vehicle for pitavastatin, was obtained from Wako Pure Chemicals (Osaka, Japan). Pitavastatin (0.1, 0.5, or 1.0 mg/kg) and CMC (0.5%) were given intravenously 12 hr or 5 min before or 12 or 24 hr after the induced transient retinal ischemia.

Morphometric Analysis

Eight eyes from 8 rats in each pitavastatin-treated, vehicle-treated, and non-operated control groups were obtained to evaluate the severity of retinal damage. Morphometric analysis was performed in a manner similar to that described previously.[16] Briefly, 7 days after the induced transient retinal ischemia, the rats were killed by an intraperitoneal overdose injection of pentobarbital and the eyes were enucleated. The eyes were immersed in a fixative containing 2.5% glutaraldehyde and 2% paraformaldehyde in 0.1 M phosphate buffer (pH 7.4) for 24 hr at 4°C, followed by dehydration and embedding in paraffin. Transverse sections 4 μm thick were made through the optic disc, were stained with hematoxylin and eosin, and were subjected to morphometric analysis. The degree of hypertension-induced neuronal damage in the retina was quantified by means of cell counts in the ganglion cell layer (GCL) and by measuring the thickness of the inner plexiform layer (IPL) and inner nuclear layer (INL), at 1.5 mm from the optic disc. Data from three sections were averaged for each eye.

Retrograde Labeling of Retinal Ganglion Cells

One day before induction of ischemia, retrograde labeling of GCL cells was performed in a manner similar to that described previously.[17] Briefly, rats were anesthetized with a 1:1 mixture of xylazine hydrochloride (4 mg/kg) and ketamine hydrochloride (10 mg/kg), and then the heads were fixed in a stereotaxic apparatus. Fluoro-Gold (Fluorochrome, Englewood, CO, USA) was microinjected bilaterally into the superior colliculus. Eight days after this injection (i.e., 7 days after the induction of ischemia), the animals were killed by an intraperitoneal overdose injection of pentobarbital and the eyes were enucleated. Eyes were fixed in 4% paraformaldehyde for 1 h. Retinas were divided into six by means of radial cuts, removed from the sclera, and mounted on slides. Fluoro-Gold GCL labeling was analyzed in a manner similar to that described previously.[17] Briefly, regions used for counting the number of GCL cells were selected from two fields in the central area (1 mm from the optic disc) from each of the six radial cuts. Thus, for each eye, 12 fields were evaluated to obtain the labeled GCL counts.

Analysis of Expression of Genes for P-Selectin and Intercellular Adhesion Molecule -1 (ICAM-1) By Real-Time Quantitative Reverse Transcription-Polymerase Chain Reaction

Seven eyes from 7 rats in each pitavastatin-treated, vehicle-treated, and non-operated control groups were

used to analyze expression of the adhesion molecules P-selectin and ICAM-1. At 12 or 24 hr after reperfusion, the eyes were enucleated and retinas were collected from posterior segments; control eyes were handled in the same fashion. Total RNA was prepared from these fresh tissue samples by using the AquaPure RNA isolation Kit (BIO-RAD, Hercules, CA, USA), according to the manufacturer's instructions. Real-time one-step reverse transcription-polymerase chain reaction (RT-PCR) was performed with SuperScript One-Step RT-PCR with Platinum Taq (Invitrogen, Carlsbad, CA, USA) by using the ABI prism 7700 Sequence Detection System (Applied Biosystems, Foster City, CA, USA), according to the manufacturer's instructions. Glyceraldehyde-3-phosphate dehydrogenase (GAPDH) was used as an internal control. For RT-PCR analysis, 1 μg of template RNA, 0.2 μM sense primers, 0.2 μM antisense primers, 1 μL of RT/Platinum Taq Mix, and 25 μL of 2× reaction mixture, in a total volume of 50 μL, were used. RNA was reverse-transcribed into cDNA by one cycle at 50°C for 30 min followed by one cycle at 94°C for 2 min. The cDNA was amplified for 40 cycles: 94°C for 15 s, 50°C for 30 s, and 72°C for 1 min (the last cycle at 72°C for 5 min). We used the primers for P-selectin, ICAM-1, and GAPDH designed by TaqMan Gene Expression Assays. Data for quantification were analyzed with the ABI PRISM 7000 analysis software. P-selectin and ICAM-1 mRNA levels were estimated as the ratio of these mRNA copies to GAPDH mRNA copies.

Statistical Analysis

All values were presented as means ± SEM. Data were analyzed via one-way analysis of variance using the post-hoc test with Fisher's protected least significant difference procedure. Differences were considered statistically significant when p values were less than 0.05.

RESULTS

Morphometric Analysis

To investigate the protective effects of pitavastatin against retinal ischemia induced by 60 min of ocular hypertension (130 mm Hg), we performed a quantitative morphometric analysis (Fig. 1). Induction of transient retinal ischemia caused severe destruction of the inner retinal elements, which led to decreased thickness of different layers and damage to retinal cells. In vehicle-treated eyes, the IPL and INL were 17.7 ± 1.1 μm and 22.8 ± 0.6 μm thick, respectively; these values were significantly lower compared with those of the control non-operated eyes, 42.3 ± 1.4 μm and 31.3 ± 1.5 μm, respectively ($p < 0.05$). In addition, the cell density of the GCL in the vehicle-treated eyes, 25.2 ± 1.7 cells/mm, was significantly reduced compared with that in the non-operated controls, 58.2 ± 3.3 cells/mm ($p < 0.05$) (Fig. 1B).

With administration of pitavastatin (0.5 mg/kg) at 5 min before the induction of transient retinal ischemia, destruction of inner retinal elements was significantly suppressed compared with control eyes (Fig. 1A). With pitavastatin treatment, the IPL and INL were 23.7 ± 2.4 μm and 25.7 ± 1.2 μm thick, respectively; both values were significantly higher than those for vehicle-treated eyes ($p < 0.05$) (Fig. 1B). Also, the cell density of the GCL in pitavastatin-treated eyes was 38.9 ± 4.5 cells/mm, which is also significantly greater than that for vehicle-treated eyes ($p < 0.05$).

Analysis of Retrograde Labeling of the GCL

To investigate whether pitavastatin protects the GCL from ischemia-reperfusion induced neuronal death, we used retrograde labeling of GCL with Fluoro-Gold, which allows the individual cells of the GCL to be observed in whole-mount retinas (Fig. 2A). The mean cell density of the GCL was 3882 ± 350 cells/mm^2 and 1725 ± 220 cells/mm^2 in controls and in vehicle-treated eyes, respectively. In contrast, the mean cell density of the GCL in pitavastatin-treated eyes was 2654 ± 302 cells/mm^2, which is significantly higher than that for the vehicle-treated eyes ($p < 0.05$) (Fig. 2B).

Dependence on Dose and Time of the Neuroprotective Effects of Pitavastatin

To elucidate possible dose-dependent relationships, different concentrations of pitavastatin (0.1, 0.5, and 1.0 mg/kg) were administered 5 min before induction of transient retinal ischemia. Our morphometric analysis showed significant differences between pitavastatin- and vehicle-treated eyes at the higher pitavastatin concentrations (Fig. 3).

To evaluate the influence of the timing of administration, pitavastatin was given at 12 hr before, at 5 min before, or at 12 or 24 hr after the induction of

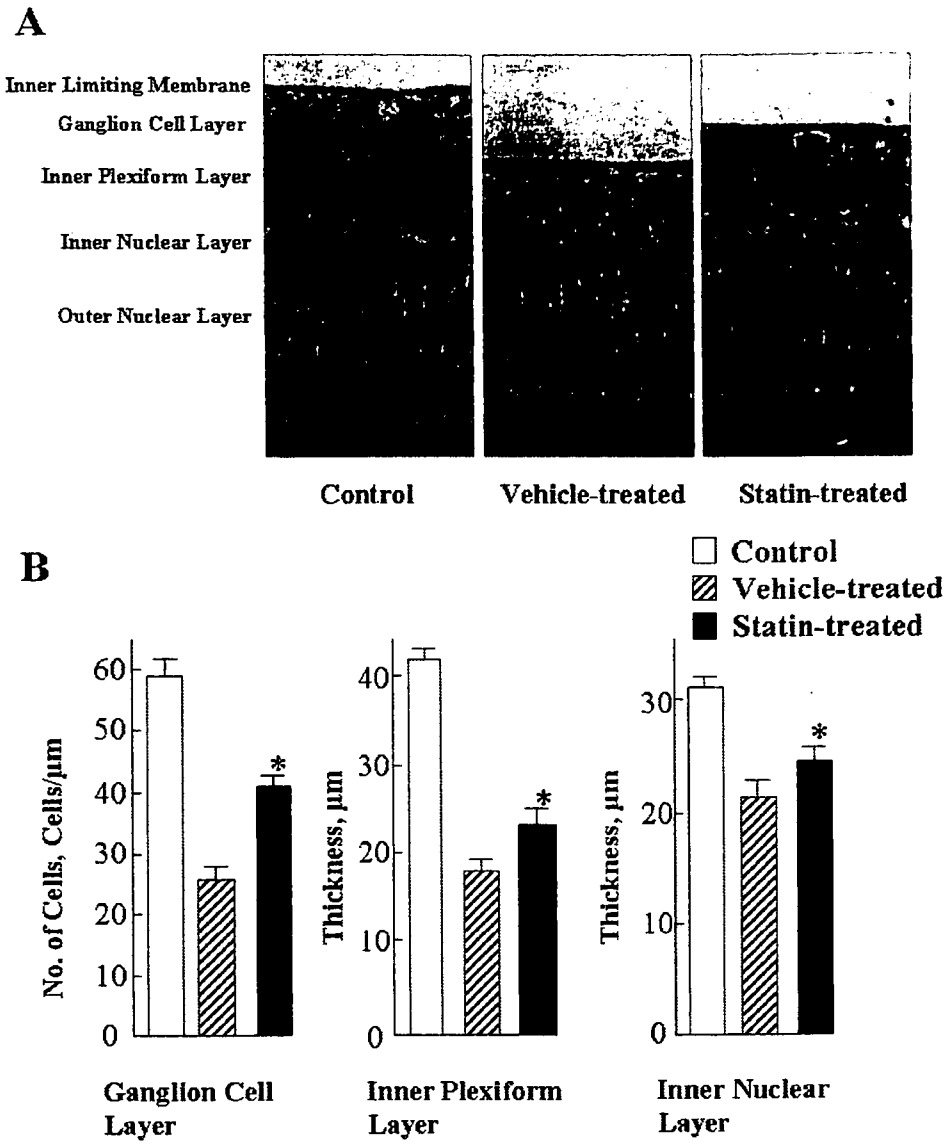

FIGURE 1 Light micrographs of the retina at a distance of 1.5 mm from the center of the optic nerve head. (A) Representative results for non-operated control, vehicle-treated, and pitavastatin-treated eyes 7 days after reperfusion. (B) Number of cells and thickness of different retinal layers at 7 days after reperfusion. Values are means ± SEM. Asterisks indicate significantly different at $p < 0.05$ compared with vehicle-treated eyes. For each group, $n = 8$.

retinal ischemia. In rats given pitavastatin at 5 min before or at 12 and 24 hr after induction of retinal ischemia, the thicknesses of the IPL and INL were significantly greater than those in vehicle-treated eyes ($p < 0.05$) (Fig. 4). In addition, the mean cell densities in the GCL in pitavastatin-treated eyes were statistically higher than those in control eyes and in vehicle-treated eyes ($p < 0.05$) (Fig. 4).

Expression of P-Selectin and ICAM-1 in the Retina

In an effort to investigate pitavastatin-mediated inhibition of a leukocyte-endothelium interaction, we performed real-time quantitative RT-PCR to determine expression levels of adhesion molecules in pitavastatin-treated or -untreated rat retinas. Figure 5 shows that ICAM-1 and P-selectin gene expression was significantly reduced at the time of 12 or 24 hr after reperfusion, which suggests that pitavastatin, like other statins, suppressed activation of endothelial cells after ischemia-reperfusion.[11,14]

DISCUSSION

The association between the long-term use of statins and ocular vascular disease has been evaluated in many clinical studies; however, the results have been

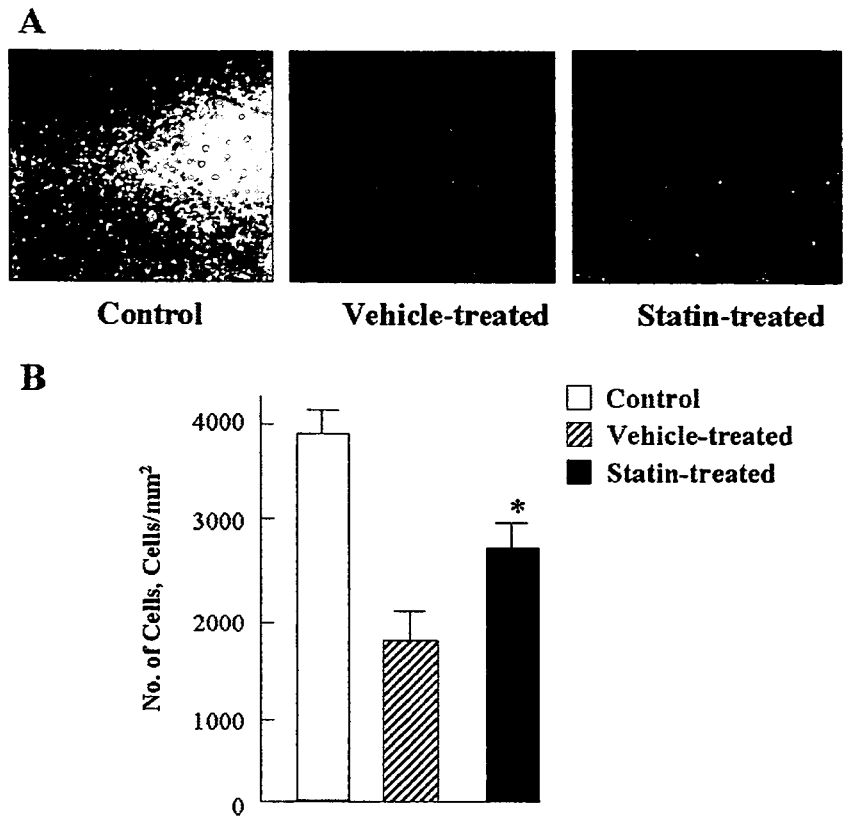

FIGURE 2 Retrograde labeling of the GCL. (A) Fluorescence microscopic photographs of representative retinal sections at 7 days after reperfusion. (B) Number of labeled cells at 7 days after reperfusion. Values are means ± SEM. Asterisks indicate significantly different at $p < 0.05$ compared with vehicle-treated eyes. For each group, $n = 7$.

contradictory.[6–9] The association between ocular diseases and statins may have two possible explanations. First, the cholesterol-lowering effects of statins and the resultant improvement in cardiovascular disease may inhibit the onset and progression of ocular disease, as evidenced by a higher incidence of cardiovascular disease in patients with AMD and diabetic retinopathy than in controls. Another possibility is that the pleiotropic effects, such as improved endothelial function, decreased low-density lipoprotein oxidation, foam cell formation, leukocyte-endothelium interactions, plaque rupture, and smooth muscle cell proliferation[18–20] of statins are therapeutic and impede the progression of retinal diseases. We previously reported that improvement of endothelial function via the pleiotropic actions of two statins, pravastatin and cerivastatin, could protect the retinal neurons against damage resulting from ischemic retina.[11] Furthermore, we recently demonstrated that the therapeutic dose of pitavastatin for human hypocholesterolemia effectively suppressed experimental choroidal neovascularization in rats via the anti-inflammatory and -angiogenic effects of pitavastatin.[13]

Pitavastatin (also known as NK-104) is a recently developed member of the statin family. This agent produces long-lasting (more than 6 hr) inhibition of liver sterol synthesis.[21] Also, its bioavailability in humans is high, with a circulating half-life of just above 13 hr, and it undergoes very slight modification by the cytochrome P450 enzyme system.[22] These characteristics suggested the possibility of long-term safety and stability of this compound in clinical situations. In addition, pitavastatin produces lower blood cholesterol and triglyceride levels at lower doses administered compared with other statins such as atorvastatin.[23,24] In addition to our previous results,[11] these data on pitavastatin encouraged us to investigate this drug as a useful therapy for retinal diseases.

Our data in the present study showed that pitavastatin had neuroprotective effects against transient retinal ischemia similar to those of two other statins, pravastatin and cerivastatin. Furthermore, our morphometric analysis revealed that even administration of pitavastatin at 24 hr after reperfusion produced neuroprotective effects similar to those obtained during the first 12 hr. Thus, administration of this drug may

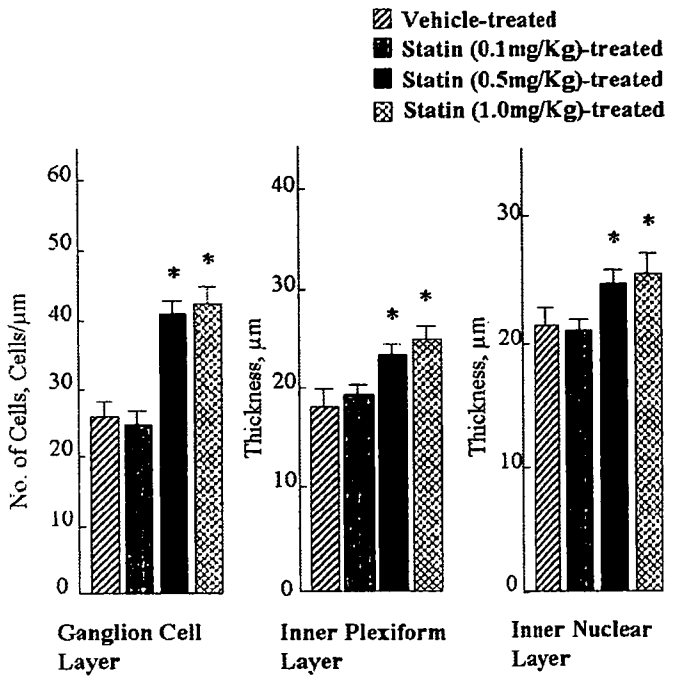

FIGURE 3 Dose dependency of the neuroprotective effects of pitavastatin. Three concentrations of pitavastatin (0.1, 0.5, and 1.0 mg/kg) were administered 5 min before induction of transient retinal ischemia. Representative results are shown for the number of cells in the GCL and the thickness of different retinal layers at 7 days after reperfusion. Values are means ± SEM. Asterisks indicate significantly different at $p < 0.05$ compared with vehicle-treated eyes. For each group, $n = 7$.

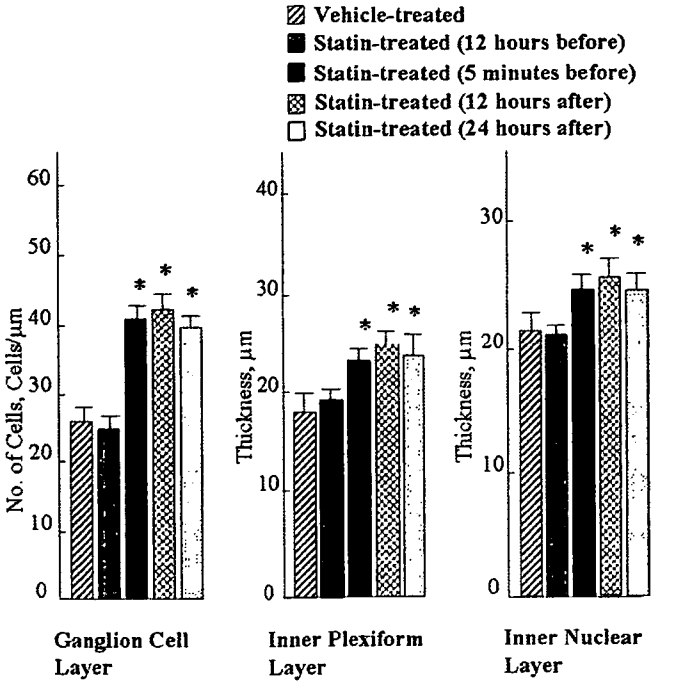

FIGURE 4 Timing of administration of pitavastatin. Pitavastatin (0.5 mg/kg) was given at 12 hr before, 5 min before, or 12 or 24 hr after the induction of transient retinal ischemia. Representative results are shown for the number of cells in the GCL and the thickness of different retinal layers at 7 days after reperfusion. Values are means ± SEM. Asterisks indicate significantly different at $p < 0.05$ compared with vehicle-treated eyes. For each group, $n = 7$.

be effective as an adjunctive treatment even after the onset of ischemic retinal disease, because it would stop progression of the disease in which the improvement of endothelial function is component of the pathogenesis.

Leukocyte adhesion molecules are reported to be upregulated during acute activation of endothelial cells induced by ischemia-reperfusion.[25] We previously clearly demonstrated that the reduction of leukocyte accumulation by inhibition of ICAM-1 and P-selectin markedly diminished the retinal damage from transient retinal ischemia in rats with pravastatin and cerivastatin.[11] In this study, we demonstrated that pitavastatin effectively reduced ICAM-1 and P-selectin expression in the retina, and protected the retina from neuronal death. These findings agree with those of our previous study.[11]

The doses of pitavastatin tested in the current study are higher than that of the normal dose in humans to treat hypercholesterolemia. However, it is generally accepted that the bioequivalent dosage must be higher, because of the higher metabolic rates in rodents. In addition, the medication is given in these animals as a single intravenous dose rather than as a sustained oral administration like human daily use. Despite these differences, our results suggested that therapeutic doses in humans may be sufficient to achieve neuroprotective action. A clinical trial would be necessary to make this determination.

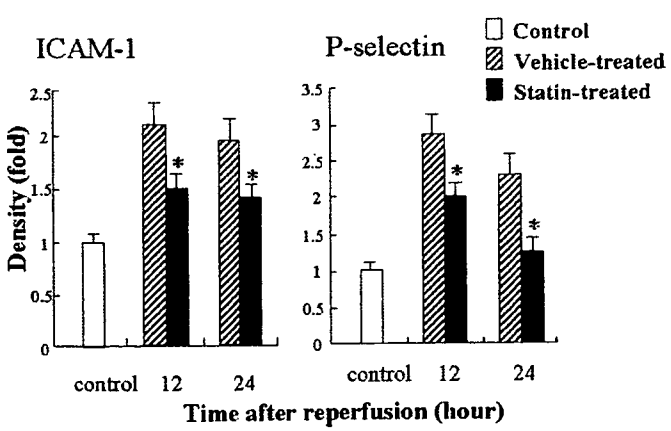

FIGURE 5 ICAM-1 and P-selectin gene expression in the retina after reperfusion. Representative results are given for ICAM-1 and P-selectin gene expression in the rat retina at 12 and 24 hr after reperfusion. ICAM-1 and P-selectin mRNA levels were estimated as the ratio of these mRNA copies to GAPDH mRNA copies. Values are means ± SEM. Asterisks indicate significantly different at $p < 0.05$ compared with vehicle-treated rats. For each group, $n = 7$.

In conclusion, our present study showed the potential of pitavastatin may have application as a novel neuroprotective treatment of ischemic retinal diseases.

ACKNOWLEDGMENTS

The authors' work was supported in part by a Grant-in-Aid for Scientific Research from the Ministry of Education, Science, Sports and Culture, Japan, and from the Ministry of Health and Welfare, Japan.

REFERENCES

[1] The Scandinavian Simvastatin Survival Study (4S). .Randomised trial of cholesterol lowering in 4444 patients with coronary heart disease. *Lancet.* 1994;344:1383–1389.

[2] Shepherd J. Statin therapy in clinical practice: new developments. *Curr Opin Lipidol.* 1995;6:254–255.

[3] Treasure CB, Klein JL, Weintraub WS, et al. Beneficial effects of cholesterol-lowering therapy on the coronary endothelium in patients with coronary artery disease. *N Engl J Med.* 1995;332:481–487.

[4] Delanty N, Vaughan CJ. Vascular effects of statins in stroke. *Stroke.* 1997;28:2315–2320.

[5] Sacks FM, Pfeffer MA, Moye LA, et al. The effect of pravastatin on coronary events after myocardial infarction in patients with average cholesterol levels. Cholesterol and recurrent events trial investigators. *N Engl J Med.* 1996;335:1001–1009.

[6] Baghdasarian SB, Jneid H, Hoogwerf BJ. Association of dyslipidemia and effects of statins on nonmacrovascular diseases. *Clin Ther.* 2004;26:337–351.

[7] Wilson HL, Schwartz DM, Bhatt HR, et al. Statin and aspirin therapy are associated with decreased rates of choroidal neovascularization among patients with age-related macular degeneration. *Am J Ophthalmol.* 2004;137:615–624.

[8] Klein R, Klein BE, Tomany SC, et al. Relation of statin use to the 5-year incidence and progression of age-related maculopathy. *Arch Ophthalmol.* 2003;121:1151–1155.

[9] McGwin G, Jr., Owsley C, Curcio CA, Crain RJ. The association between statin use and age related maculopathy. *Br J Ophthalmol.* 2003;87:1121–1125.

[10] McGwin G, Jr, McNeal S, Owsley C, et al. Statins and other cholesterol-lowering medications and the presence of glaucoma. *Arch Ophthalmol.* 2004;122:822–826.

[11] Honjo M, Tanihara H, Nishijima K, et al. Statin inhibits leukocyte-endothelial interaction and prevents neuronal death induced by ischemia-reperfusion injury in the rat retina. *Arch Ophthalmol.* 2002;120:1707–1713.

[12] Zambarakji HJ, Nakazawa T, Connolly E, et al. Dose-dependent effect of pitavastatin on VEGF and angiogenesis in a mouse model of choroidal neovascularization. *Invest Ophthalmol Vis Sci.* 2006;47:2623–2631.

[13] Sagara N, Kawaji T, Takano A, et al. Effect of pitavastatin on experimental choroidal neovascularization in rats. *Exp Eye Res.* 2007;84:1074–1080.

[14] Miyahara S, Kiryu J, Yamashiro K, et al. Simvastatin inhibits leukocyte accumulation and vascular permeability in the retinas of rats with streptozotocin-induced diabetes. *Am J Pathol.* 2004;164:1697–1706.

[15] Rosenbaum DM, Rosenbaum PS, Gupta A, et al. Retinal ischemia leads to apoptosis which is ameliorated by aurintricarboxylic acid. *Vision Res.* 1997;37:3445–3451.

[16] Morizane C, Adachi K, Furutani I, et al. N(omega)-nitro-L-arginine methyl ester protects retinal neurons against N-methyl-D-aspartate-induced neurotoxicity in vivo. *Eur J Pharmacol.* 1997;328:45–49.

[17] Sawada A, Neufeld AH. Confirmation of the rat model of chronic, moderately elevated intraocular pressure. *Exp Eye Res.* 1999;69:525–531.

[18] Rosenson RS, Tangney CC. Antiatherothrombotic properties of statins: implications for cardiovascular event reduction. *JAMA.* 1998;279:1643–1650.

[19] Laufs U, Liao JK. Direct vascular effects of HMG-CoA reductase inhibitors. *Trends Cardiovasc Med.* 2000;10:143–148.

[20] Takemoto M, Liao JK. Pleiotropic effects of 3-hydroxy-3-methylglutaryl coenzyme A reductase inhibitors. *Arterioscler Thromb Vasc Biol.* 2001;21:1712–1719.

[21] Aoki T, Nishimura H, Nakagawa S, et al. Pharmacological profile of a novel synthetic inhibitor of 3-hydroxy-3-methylglutaryl-coenzyme A reductase. *Arzneimittelforschung.* 1997;47:904–909.

[22] Kojima J, Fujino H, Abe H, et al. Identification of metabolites of NK-104, an HMG-CoA reductase inhibitor, in rat, rabbit and dog bile. *Biol Pharm Bull.* 1999;22:142–150.

[23] Kajinami K, Koizumi J, Ueda K, et al. Effects of NK-104, a new hydroxymethylglutaryl-coenzyme reductase inhibitor, on low-density lipoprotein cholesterol in heterozygous familial hypercholesterolemia. Hokuriku NK-104 Study Group. *Am J Cardiol.* 2000;85:178–183.

[24] Saito Y, Yamada N, Teramoto T, et al. Clinical efficacy of pitavastatin, a new 3-hydroxy-3-methylglutaryl coenzyme A reductase inhibitor, in patients with hyperlipidemia. Dose-finding study using the double-blind, three-group parallel comparison. *Arzneimittelforschung.* 2002;52:251–255.

[25] Kubes P, Suzuki M, Granger DN. Nitric oxide: an endogenous modulator of leukocyte adhesion. *Proc Natl Acad Sci USA.* 1991;88:4651–4655.

Manuscript (All Manuscript Text Pages in MS Word format, includi

Long-Term Relationship between Intraocular Pressure and Visual Field Loss in Primary Open-Angle Glaucoma

Masaru Inatani,[1] Keiichiro Iwao,[1] Toshihiro Inoue,[1] Maiko Awai,[1] Takahito Muto,[1] Takahisa Koga,[1] Minako Ogata-Iwao,[2] Ryuhei Hara,[2] Ryusuke Futa,[2] Hidenobu Tanihara[1]

[1]Department of Ophthalmology and Visual Science, Kumamoto University Graduate School of Medical Sciences, Kumamoto, Japan, and [2]Department of Ophthalmology, Nippon Telegraph and Telephone Corporation West Kyushu General Hospital.

Corresponding author; Masaru Inatani

Department of Ophthalmology and Visual Science, Kumamoto University Graduate School of Medical Sciences, 1-1-1, Honjo, 860-8556 Kumamoto, Japan

E-mail: inatani@fc.kuh.kumamoto-u.ac.jp

Tel.: +81-96-373-5247

Fax: +81-96-373-5249

Statement of conflict of interest: none

This study was supported, in part, by Grants-in-Aid for Scientific Research from the Ministry of Education, Science, Sports and Culture of Japan, and from the Ministry of Health and Welfare of Japan.

Abstract

Purpose: To investigate the dependence upon intraocular pressure of the progression of visual field defects in eyes with primary open-angle glaucoma, in which the mean intraocular pressure was maintained at <21 mmHg.

Methods: This study involved 100 eyes with primary open-angle glaucoma, which were followed up for ≥5 years. The mean intraocular pressure levels were maintained at <21 mmHg during the follow-up period. The relationship between the intraocular pressure and the progression of visual field defects, which was scored using the Advanced Glaucoma Intervention Study criteria, was investigated retrospectively.

Results: Compared with the baseline scores, the visual field defect scores had significantly worsened by the end of the follow-up period (p<0.0001, Wilcoxon paired signed rank test). The change in the visual field defect score (2.5±0.5) in eyes with average intraocular pressure levels of ≥16 mmHg (n=36) was significantly greater (p=0.031, Mann Whitney-U test) than the change (1.3±0.3) in eyes with average intraocular pressure levels of <16 mmHg (n=64). Moreover, intraocular pressures of ≥18 mmHg made a major contribution to the aggravation of visual field defects in eyes with primary open-angle glaucoma.

Conclusions: Eyes with primary open-angle glaucoma and with mean intraocular pressure levels maintained at <21 mmHg underwent intraocular pressure-dependent progression of their visual field defects. Our results suggest that further intraocular pressure-lowering would be beneficial in such cases.

Key words: Advanced Glaucoma Intervention Study; cupping/disc ratio; Humphrey visual field analyzer; normal tension glaucoma